Slow dynamics of linear relaxation systems

ARTICLE *in* PHYSICA A: STATISTICAL MECHANICS AND ITS APPLICATIONS · NOVEMBER 1994

Impact Factor: 1.73 · DOI: 10.1016/0378-4371(94)00187-1

2 AUTHORS:

Bogdan Cichocki
University of Warsaw
140 PUBLICATIONS **2,512** CITATIONS
SEE PROFILE

Ubbo Felderhof
RWTH Aachen University
420 PUBLICATIONS **6,036** CITATIONS
SEE PROFILE

ELSEVIER

Physica A 211 (1994) 165–192

PHYSICA A

Slow dynamics of linear relaxation systems

B. Cichocki [a,b], B.U. Felderhof [c]

[a] *Institute of Theoretical Physics, Warsaw University, Hoza 69, 00-618 Warsaw, Poland*

[b] *Institute of Fundamental Technological Research, Polish Academy of Sciences, Świętokrzyska 21, 00-049 Warsaw, Poland*

[c] *Institut für Theoretische Physik A, R.W.T.H. Aachen, Templergraben 55, 52056 Aachen, Germany*

Received 27 June 1994

Abstract

Linear relaxation, occurring in dielectrics, viscoelastic fluids, and many other systems, is often characterized by a broad continuous spectrum. We show that the relaxation behavior may be analyzed effectively by means of N-point Padé approximants, applied in the complex plane of the square root of frequency. The method leads to a compact analytic expression for the Laplace transform of the relaxation function, characterized by a small number of poles and their residues in the square root of frequency plane. We study the method in detail for a model of diffusion in three dimensions with a single or double radial potential barrier, and demonstrate its use in the analysis of the viscoelastic relaxation spectrum of polyisobutylene.

1. Introduction

Linear response theory deals with the reaction of a system to applied forces or fields of amplitude sufficiently small that the superposition principle applies. Usually the admittance function characterizing the response has a memory character. The mathematical theory of linear response has been developed in depth by König and Meixner [1–3]. They coined the term linear passive systems, and gave a precise mathematical definition. The microscopic statistical mechanical theory of linear response of a physical system was first formulated by Kubo [4,5].

The theory of linear response finds application in many branches of science and technology. It provides a general framework exhibiting interesting connections between seemingly unrelated disciplines. It was shown by Meixner [6] that electrical networks furnish an excellent example for the application of thermodynamics of irreversible processes. Linear mechanical systems with damping can also be modeled as electrical networks.

SSDI 0378-4371(94)00187-1

In the following we study a particular class of linear passive systems, so-called relaxation systems [2,7]. These systems are purely damped, and are characterized by a spectrum of relaxation times. Examples are *RC* and *RL* electrical networks, viscoelasticity [8], dielectric relaxation [9], magnetic relaxation, and chemical reactions. Often the relaxation spectrum is continuous and very broad. There are many phenomenological equations which provide an approximate description of the frequency-dependence of the linear response in viscoelasticity [8] or in dielectric relaxation [9]. Any proposed equation may be characterized by its corresponding relaxation spectrum.

It has been suggested by Kauzmann [10] that the reason for the broad continuous spectrum in dielectric relaxation is a wide distribution of activation energies for molecular motion. The hole theory of Eyring [11] proposes a similar reason for the broad spectrum in viscoelasticity by assuming a distribution of jump rates. Kramers' theory of reaction rates [12–16] shows that the underlying mechanism can be understood as a diffusion process in a generalized coordinate space. Since we are dealing with linear relaxation systems in Meixner's sense, we are concerned only with Kramers' theory of Brownian motion in the overdamped limit. The statistical theory may be formulated on the basis of a Smoluchowski equation for the probability distribution in a generalized coordinate space [13,14].

A typical example of the phenomenological description of frequency-dependent response is the Barlow–Erginsav–Lamb expression [17] for the dynamic shear viscosity of a liquid. This has the form

$$\eta(\omega) = \eta(0)\left[1 + \sigma\sqrt{-i\omega\tau_M} - i\omega\tau_M\right]^{-1} \qquad \text{(BEL)}, \tag{1.1}$$

where $\eta(0)$ is the zero frequency shear viscosity, σ is a numerical parameter, and τ_M is the Maxwell relaxation time. The latter is given by $\tau_M = \eta(0)/G_\infty$, where G_∞ is the high-frequency shear modulus. Experiments on many supercooled liquids [18] are described by the simple BEL equation (1.1) with the universal value $\sigma = 2$. Experiments on many mixtures may be described by the same equation with a different value for the parameter [19]. The latter determines the amplitude of the long-time tail of the stress relaxation function [20]. The distribution of relaxation rates u/τ_M, corresponding to Eq. (1.1), is

$$p(u) = \frac{1}{\pi}\frac{\sigma\sqrt{u}}{1 + (\sigma^2 - 2)u + u^2}. \tag{1.2}$$

The distribution tends to a delta-function for $\sigma \to 0$, and broadens with increasing σ. An expression like Eq. (1.1) with $\sigma = 2$ also describes the bulk viscosity of many liquids [18]. A similar expression holds for the velocity relaxation function describing the time-dependent mean square displacement of a selected particle in a suspension of interacting Brownian particles [21–23].

The BEL equation (1.1) has particular standing in the mathematical theory of relaxation systems. It is the simplest possible form having a square-root dependence at low frequency and an inverse dependence at high frequency. The value $\sigma = 2$ is special, because for this value the two poles in the $\sqrt{\omega}$ plane coalesce. In the following we are

concerned with a natural generalization of the BEL equation involving a larger number of poles.

In Section 2 we formulate the generalized Smoluchowski equation and define the relaxation spectrum of a general time-correlation function. In the following sections we study diffusion in a spherically symmetric potential as a simple model exhibiting the essential features. We show that a single barrier leads to a relaxation spectrum which is well approximated by a two-pole expression, as in Eq. (1.1). Corrections require a larger number of poles. In a double barrier model the two-pole expression fails, if the wells are sufficiently deep or the barriers sufficiently high. At least four poles in the $\sqrt{\omega}$ plane are required to furnish an adequate description.

We show that the method of N-point Padé approximants [24,25] provides a suitable mathematical framework for the description of linear relaxation systems. In our model calculations the method allows an accurate representation of the relaxation spectrum in simple mathematical form. In Section 10 we show that the method can be used successfully in the interpretation of experimental data.

2. Smoluchowski equation

We consider a system whose dynamics on a slow time scale may be characterized as diffusion in a generalized coordinate space. Let the configuration be given by the N-dimensional vector $\boldsymbol{X}$. The dynamical evolution of the configuration is assumed to be described by a time-dependent probability distribution $P(\boldsymbol{X}, t)$, which obeys the generalized Smoluchowski equation [13,14]. In abbreviated form this reads

$$\frac{\partial P}{\partial t} = \mathcal{D} P, \tag{2.1}$$

where $\mathcal{D}$ is the Smoluchowski operator defined by

$$\mathcal{D} P = \frac{\partial}{\partial \boldsymbol{X}} \cdot \boldsymbol{D} \cdot \left[\frac{\partial P}{\partial \boldsymbol{X}} + \beta \frac{\partial \Phi}{\partial \boldsymbol{X}} P \right]. \tag{2.2}$$

Here $\boldsymbol{D}(\boldsymbol{X})$ is the $N \times N$ diffusion matrix, which may depend on configuration. Furthermore, $\beta = 1/k_B T$ and $\Phi(\boldsymbol{X})$ is a configuration-dependent potential. We assume that the configuration space is bounded. Then the Smoluchowski equation (2.1) describes how the function $P(\boldsymbol{X}, t)$ tends to the equilibrium distribution

$$P_{eq}(\boldsymbol{X}) = \exp\left[-\beta \Phi(\boldsymbol{X})\right] / Z(\beta) \tag{2.3}$$

in the course of time. The partition function $Z(\beta)$ normalizes the distribution to unity.

We write the distribution function as

$$P(\boldsymbol{X}, t) = f(\boldsymbol{X}, t) P_{eq}(\boldsymbol{X}). \tag{2.4}$$

The function $f(\boldsymbol{X}, t)$ satisfies the equation

$$\frac{\partial f}{\partial t} = \mathcal{L} f, \tag{2.5}$$

with the adjoint Smoluchowski operator

$$\mathcal{L} = \left[\frac{\partial}{\partial \boldsymbol{X}} - \beta \frac{\partial \Phi}{\partial \boldsymbol{X}}\right] \cdot \boldsymbol{D} \cdot \frac{\partial}{\partial \boldsymbol{X}}. \tag{2.6}$$

If $A(\boldsymbol{X})P_{eq}(\boldsymbol{X})$ is the initial distribution function, then the one-sided Fourier transform

$$\hat{f}(\boldsymbol{X}, \omega) = \int_0^\infty e^{i\omega t} f(\boldsymbol{X}, t)\, dt \tag{2.7}$$

satisfies

$$(i\omega + \mathcal{L})\hat{f} = -A. \tag{2.8}$$

It is of interest to consider the correlation function

$$C_A(t) = \int A^*(\boldsymbol{X}) f(\boldsymbol{X}, t) P_{eq}(\boldsymbol{X})\, d\boldsymbol{X}. \tag{2.9}$$

Here it is convenient to generalize to complex functions $A(\boldsymbol{X})$. The Fourier transform $\hat{C}_A(\omega)$ can be written as

$$\hat{C}_A(\omega) = -\langle A^*(i\omega + \mathcal{L})^{-1} A\rangle \tag{2.10}$$

with the notation

$$\langle B\rangle = \int B(\boldsymbol{X}) P_{eq}(\boldsymbol{X})\, d\boldsymbol{X}. \tag{2.11}$$

The Fourier transform has the asymptotic behavior

$$\hat{C}_A(\omega) \approx \frac{-\langle A^* A\rangle}{i\omega} \qquad \text{as } \omega \to \infty, \tag{2.12}$$

corresponding to the initial value

$$C_A(0) = \langle A^* A\rangle. \tag{2.13}$$

We define the mean relaxation time

$$\tau_M = \frac{1}{C_A(0)} \int_0^\infty C_A(t)\, dt. \tag{2.14}$$

It may be expressed as

$$\tau_M = \frac{-\langle A^* \mathcal{L}^{-1} A\rangle}{\langle A^* A\rangle}. \tag{2.15}$$

We write the correlation function as

$$C_A(t) = C_A(0)\gamma_A(t/\tau_M). \tag{2.16}$$

It follows from the general properties of the Smoluchowski equation [13,14] that the dimensionless function $\gamma_A(\tau)$ may be expressed as

$$\gamma_A(\tau) = \int_0^\infty p_A(u)\, e^{-u\tau}\, du, \tag{2.17}$$

with a spectral density $p_A(u)$ which has been normalized to

$$\int_0^\infty p_A(u) du = 1, \qquad \int_0^\infty \frac{p_A(u)}{u}\, du = 1. \tag{2.18}$$

The correlation function $C_A(t)$ decays monotonically with time. In fact, it is a completely monotone function [26], i.e. for any time t its successive derivatives alternate in sign.

The Fourier transform $\hat{C}_A(\omega)$ may be expressed as

$$\hat{C}_A(\omega) = \langle A^* A \rangle\, \tau_M \Gamma_A(z), \tag{2.19}$$

where $\Gamma_A(z)$ is the Laplace transform of the function $\gamma_A(\tau)$,

$$\Gamma_A(z) = \int_0^\infty e^{-z\tau}\, \gamma_A(\tau) d\tau, \tag{2.20}$$

with the variable $z = -i\omega\tau_M$. Substituting Eq. (2.17) we find that $\Gamma_A(z)$ is given by the Stieltjes integral

$$\Gamma_A(z) = \int_0^\infty \frac{p_A(u)}{u + z}\, du. \tag{2.21}$$

Thus $\Gamma_A(z)$ is analytic in the complex z plane with singularities on the negative real z axis. From the normalization properties Eq. (2.18) it follows that

$$\Gamma_A(0) = 1, \qquad \Gamma_A(z) \approx \frac{1}{z} \qquad \text{as } z \to \infty. \tag{2.22}$$

In many cases the relaxation function $\gamma_A(\tau)$ decays with a fractional power law for large τ in the thermodynamic limit. In such a case an expansion of $\Gamma_A(z)$ in powers of z does not exist, and the function has a branch cut along the negative z axis.

3. Diffusion in a potential

As a model for our theory of relaxation we consider a single particle diffusing in a three-dimensional radially symmetric potential $v(r)$. The position of the particle may be regarded as a reaction coordinate. The diffusion coefficient will be taken to be a constant D_0. The Smoluchowski equation for the distribution $P(\boldsymbol{r}, t)$ reads

$$\frac{\partial P}{\partial t} = D_0 \nabla \cdot \left[\nabla P + \beta(\nabla v) P\right]. \tag{3.1}$$

The potential is assumed to vanish beyond a cutoff distance r_c, so that the particle can diffuse towards infinity. As a consequence, the Smoluchowski equation (3.1) does not have a genuine equilibrium solution. On the other hand, the radial function

$$g(r) = \exp[-\beta v(r)] \tag{3.2}$$

is a time-independent solution. If we write the distribution function as

$$P(\boldsymbol{r},t) = f(\boldsymbol{r},t)g(r), \tag{3.3}$$

then the function $f(\boldsymbol{r},t)$ satisfies an equation of the form (2.5) with the adjoint Smoluchowski operator

$$\mathcal{L} = D_0[\nabla - \beta(\nabla v)] \cdot \nabla. \tag{3.4}$$

We can apply the formalism of the preceding section with $P_{eq}(\boldsymbol{X})$ replaced by $g(r)$. We do not require that the function $P(\boldsymbol{r},t)$ be normalized to unity.

We consider in particular a radial function $A(r)$ and the corresponding initial value $f(r,0) = A(r)$. The initial value of the correlation function is given by

$$C_A(0) = 4\pi \int_0^\infty |A(r)|^2 g(r) r^2 \, dr. \tag{3.5}$$

The calculation of the mean relaxation time from Eq. (2.15) requires solution of the steady-state equation

$$D_0 \left[\nabla^2 f^{(0)} - \beta \frac{dv}{dr}\frac{df^{(0)}}{dr}\right] = -A(r). \tag{3.6}$$

The mean relaxation time is given by

$$\tau_M = 4\pi \int_0^\infty A^*(r) f^{(0)}(r) g(r) r^2 \, dr \, / C_A(0). \tag{3.7}$$

Its value depends on the details of the steady-state solution $f^{(0)}(r)$. We can rewrite Eq. (3.6) as

$$D_0 \nabla \cdot [g \nabla f^{(0)}] = -gA. \tag{3.8}$$

This shows that $f^{(0)}(r)$ may be interpreted as the electrostatic potential generated by the charge density $g(r)A(r) \, / 4\pi D_0$ in a medium with dielectric constant $g(r)$. If $A(r)$ vanishes for $r > r_c$, then the solution $f^{(0)}(r)$ decays for $r > r_c$ as Q_A/r. The asymptotic coefficient Q_A is given by

$$Q_A = \frac{1}{D_0} \int_0^\infty A(r) g(r) r^2 \, dr. \tag{3.9}$$

We shall show that it may be related to the amplitude of the long-time decay of the correlation function $C_A(t)$.

The one-sided Fourier transform $\hat{f}(r,\omega)$ of the function $f(r,t)$ satisfies the radial equation

$$\frac{d^2\hat{f}}{dr^2} + \left(\frac{2}{r} - \beta\frac{dv}{dr}\right)\frac{d\hat{f}}{dr} + \frac{i\omega}{D_0}\hat{f} = -\frac{1}{D_0}A(r). \tag{3.10}$$

We transform to dimensionless form by use of the variable $x = r/a$, where a is a characteristic distance. The radial equation becomes

$$\frac{d^2\hat{f}}{dx^2} + \left(\frac{2}{x} - \beta\frac{dv}{dx}\right)\frac{d\hat{f}}{dx} - \alpha^2\hat{f} = -\frac{a^2}{D_0}A, \tag{3.11}$$

with the variable

$$\alpha^2 = -i\omega a^2/D_0. \tag{3.12}$$

We write Eq. (3.11) as

$$[\mathcal{L}_x - \alpha^2]\hat{f} = -\frac{a^2}{D_0}A. \tag{3.13}$$

The expression (2.10) for the Fourier transform $\hat{C}_A(\omega)$ may be reduced to a one-dimensional integral

$$\hat{C}_A(\omega) = 4\pi a^3 \int_0^\infty x^2 g A^* \hat{f}\, dx. \tag{3.14}$$

Introducing the scalar product

$$(A|B) = \int_0^\infty x^2 g A^* B\, dx \tag{3.15}$$

we may also write the formal expression

$$\hat{C}_A(\omega) = -\frac{4\pi a^5}{D_0}(A|\frac{1}{\mathcal{L}_x - \alpha^2}|A). \tag{3.16}$$

The operator $\mathcal{L}_x$ is Hermitian with respect to the scalar product (3.15).

4. Long-time behavior

The long-time behavior of the correlation function $C_A(t)$ is related to the behavior of its Fourier transform $\hat{C}_A(\omega)$ at low frequency. Under mild conditions on the potential $v(r)$ the solution $\hat{f}(x,\alpha)$ of Eq. (3.13) will be analytic in the complex variable α, defined such that $\alpha = (1-i)\sqrt{\omega a^2/2D_0}$ for $\omega > 0$. Thus we write

$$\hat{f}(x,\alpha) = f^{(0)}(x) + f^{(1)}(x)\alpha + f^{(2)}(x)\alpha^2 + O(\alpha^3), \tag{4.1}$$

where $f^{(0)}(x)$ is the solution of the steady-state Eq. (3.6). It follows from Eq. (3.14) that the Fourier transform $\hat{C}_A(\omega)$ has the corresponding expansion

$$\hat{C}_A(\omega) = \hat{C}_A(0) + C_A^{(1)}\alpha + C_A^{(2)}\alpha^2 + O(\alpha^3). \tag{4.2}$$

The first coefficient is related to the mean relaxation time. From Eq. (2.14) we find

$$\tau_M = \hat{C}_A(0) \,/\, C_A(0), \tag{4.3}$$

which may be expressed in the form (3.7). The next coefficient $C_A^{(1)}$ determines the amplitude of the long-time tail of the correlation function $C_A(t)$. For large t one finds

$$C_A(t) = -\frac{C_A^{(1)}\sqrt{\tau_0}}{2\sqrt{\pi}}\, t^{-3/2} + O(t^{-2}), \tag{4.4}$$

where $\tau_0 = a^2/D_0$. We shall show that the coefficient $C_A^{(1)}$ may be calculated easily.

It follows from Eq. (3.13) that beyond the cutoff distance $x_c = r_c/a$ the solution $\hat{f}(x,\alpha)$ takes the form

$$\hat{f}(x,\alpha) = \gamma(\alpha)\frac{e^{-\alpha x}}{x} \qquad \text{for } x > x_c, \tag{4.5}$$

with a coefficient $\gamma(\alpha)$ which has the expansion

$$\gamma(\alpha) = \gamma^{(0)} + \gamma^{(1)}\alpha + O(\alpha^2). \tag{4.6}$$

By comparison with the steady-state solution $f^{(0)}(x)$

$$\gamma^{(0)} = Q_A/a. \tag{4.7}$$

By substitution of the expansion (4.1) into Eq. (3.13) we see that $f^{(1)}(x)$ is a solution of the homogeneous equation

$$\mathcal{L}_x f^{(1)} = 0. \tag{4.8}$$

Hence $f^{(1)}(x)$ must be a constant. By comparison with Eq. (4.5)

$$\gamma^{(1)} = 0, \qquad f^{(1)}(x) = -\gamma^{(0)}. \tag{4.9}$$

From Eqs. (3.9), (3.14), and (4.1) we therefore find

$$C_A^{(1)} = -4\pi\frac{D_0}{a}|Q_A|^2. \tag{4.10}$$

The value of Q_A is found from the simple quadrature (3.9). Note that the coefficient $C_A^{(1)}$ is always negative. Using earlier notation [21] we write

$$\sigma = -\frac{C_A^{(1)}\sqrt{\tau_0}}{C_A(0)\tau_M^{3/2}}. \tag{4.11}$$

We have called σ the width parameter, since it may be related to the width of the spectral density $p_A(u)$. The mean relaxation time τ_M sets the overall time scale, the parameter σ is a measure of the spread of relaxation times.

5. Single barrier

We have shown previously in the problem of self-diffusion [21–23] that a simple approximation to the relaxation function $\gamma_A(\tau)$ often provides a good description. We have called the approximation the two-pole approximation, because the Laplace transform $\Gamma_A(z)$, defined in Eq. (2.20), is approximated by a function with two simple poles in the $\sqrt{z}$ plane. Explicitly the two-pole approximation reads

$$\Gamma_{A2}(z) = \frac{1}{1+\sigma\sqrt{z}+z}. \tag{5.1}$$

This is just the factor appearing in the BEL equation (1.1). In order to construct the approximation one must find the initial value $C_A(0)$, the mean relaxation time τ_M, and the width parameter σ. In two-pole approximation the spectral density $p_A(u)$, defined in Eq. (2.17), is approximated by

$$p_{A2}(u) = \frac{1}{\pi}\frac{\sigma\sqrt{u}}{1+(\sigma^2-2)u+u^2}, \tag{5.2}$$

the same expression as in Eq. (1.2). We shall investigate to what extent the two-pole approximation adequately describes the process of diffusion across a single barrier.

To obtain explicit results we consider a simple model with potential given by

$$\begin{aligned} v(r) &= v_0 \quad \text{for } 0 < r < a, \\ &= v_1 \quad \text{for } a < r < b, \\ &= 0 \quad \text{for } b < r. \end{aligned} \tag{5.3}$$

The heights v_0 and v_1 may be positive as well as negative. Usually we take v_0 negative and v_1 positive, corresponding to a well for $0 < r < a$, separated from free space by a barrier for $a < r < b$. We consider the function

$$A(r) = \theta(a-r), \tag{5.4}$$

corresponding to an initial distribution which is uniform in the well and zero elsewhere. From Eq. (3.5) the initial value of the correlation function is given by

$$C_A(0) = \frac{4\pi}{3}a^3 g_0, \tag{5.5}$$

with $g_0 = \exp(-\beta v_0)$. From Eq. (3.8) we see that the radial function $f^{(0)}(r)$ must satisfy the jump conditions

$$\begin{aligned} &f^{(0)}(x_j+) = f^{(0)}(x_j-) \\ &g_{j+1} f^{(0)'}(x_j+) = g_j f^{(0)'}(x_j-), \qquad j = 0, 1, \end{aligned} \tag{5.6}$$

with $x_0 = 1$, $x_1 = b/a$, and $g_1 = \exp(-\beta v_1)$, $g_2 = 1$. Hence one finds

$$\frac{1}{\tau_0} f^{(0)}(x) = -\tfrac{1}{6}x^2 + X_0^{(0)}, \quad 0 < x < 1,$$

$$= X_1^{(0)} + \frac{Y_1^{(0)}}{x}, \quad 1 < x < x_1,$$

$$= \frac{Y_2^{(0)}}{x}, \quad x_1 < x, \tag{5.7}$$

with coefficients

$$X_0^{(0)} = \tfrac{1}{6} + \frac{g_0}{3g_1x_1}(g_1 + x_1 - 1),$$

$$X_1^{(0)} = \frac{g_0}{3g_1x_1}(g_1 - 1),$$

$$Y_1^{(0)} = \frac{g_0}{3g_1}, \qquad Y_2^{(0)} = \tfrac{1}{3}g_0. \tag{5.8}$$

From Eq. (3.7) we find for the mean relaxation time

$$\tau_M = \left[X_0^{(0)} - \tfrac{1}{10}\right]\tau_0. \tag{5.9}$$

For zero potential $X_0^{(0)} = \frac{1}{2}$, and the mean relaxation time takes the value $\tau_{M0} = \frac{2}{5}\tau_0$. From Eq. (3.9) we find for the "charge" Q_A

$$Q_A = \tfrac{1}{3}g_0\tau_0 a, \tag{5.10}$$

which agrees with the value for $Y_2^{(0)}$ in Eq. (5.8). From Eqs. (4.10) and (4.11) we find for the parameter σ

$$\sigma = \tfrac{1}{3}g_0\left(\frac{\tau_0}{\tau_M}\right)^{3/2}. \tag{5.11}$$

For zero potential the parameter takes the value $\sigma_0 = 1.318$, corresponding to a broad spectrum.

It is of interest to consider the limiting case $g_1 << 1$, corresponding to a high barrier. The mean relaxation time is approximately

$$\tau_M \approx \frac{g_0}{3g_1}\frac{b-a}{b}\tau_0, \tag{5.12}$$

which shows dependence on v_1 of Arrhenius type. If g_0 and $x_1 - 1$ are of order unity, then $\tau_M >> \tau_0$. In this case σ is small, and the correlation function decays almost exponentially. The mean relaxation time can be identified with the escape rate.

More generally we can compare the mean relaxation time with the mean exit time [13,14]. For each starting point inside a sphere of radius $b+$ we can evaluate the average time it takes to pass through the sphere surface for the first time. For starting point at radius $r = xa$ the average time is given by the solution $f_e(x)$ of the equation

$$\mathcal{L}_x f_e = -\tau_0 \qquad \text{for } 0 < x < x_1+, \tag{5.13}$$

with absorbing boundary condition at x_1+, i.e. $f_e(x_1+) = 0$. The solution is

$$f_e(x) = \left[\tfrac{1}{6}(x_1^2 - x^2) + \frac{g_0 - g_1}{3g_1x_1}(x_1 - 1)\right]\tau_0 \qquad \text{for } 0 < x < 1. \tag{5.14}$$

Averaging over the sphere of radius a we find the mean exit time

$$\tau_{e1} = \left[\tfrac{1}{6}x_1^2 + \frac{g_0 - g_1}{3g_1 x_1}(x_1 - 1) - \tfrac{1}{10}\right]\tau_0. \tag{5.15}$$

In the limiting case $g_1 << 1$ this becomes identical with the mean relaxation time τ_M. More generally there can be a distinct difference, since the correlation function includes processes in which the particle crosses the barrier any number of times.

For the present simple model the correlation function $C_A(t)$ can be evaluated exactly, so that we can investigate the quality of the two-pole approximation (5.1). The radial equation (3.11) is easily solved on each interval, where the potential is constant. At the points of discontinuity the solution $\hat{f}(x,\alpha)$ must satisfy jump conditions of the form (5.6). One finds

$$\begin{aligned}\frac{1}{\tau_0}\hat{f}(x,\alpha) &= \frac{1}{\alpha^2} + X_0 i_0(\alpha x) && 0 < x < 1,\\ &= X_1 i_0(\alpha x) + Y_1 k_0(\alpha x) && 1 < x < x_1,\\ &= Y_2 k_0(\alpha x) && x_1 < x,\end{aligned} \tag{5.16}$$

with modified spherical Bessel functions [27]

$$i_0(z) = \frac{\sinh z}{z}, \qquad k_0(z) = \frac{e^{-z}}{z}. \tag{5.17}$$

The coefficients are given by

$$\begin{aligned}X_0 &= \frac{-1}{\alpha^2 i_0} + X_1 + \frac{k_0}{i_0}Y_1,\\ X_1 &= g_0(1-g_1)\frac{i_1\hat{k}_0\hat{k}_1}{\alpha^2\Delta},\\ Y_1 &= -g_0\frac{i_1(\hat{i}_0\hat{k}_1 + g_1\hat{i}_1\hat{k}_0)}{\alpha^2\Delta},\\ Y_2 &= -\frac{g_0 g_1 i_1}{\alpha^4 x_1^2\Delta},\end{aligned} \tag{5.18}$$

with denominator

$$\Delta = (g_0 - g_1)(1-g_1)i_0 i_1\hat{k}_0\hat{k}_1 - (g_0 i_1 k_0 + g_1 i_0 k_1)(\hat{i}_0\hat{k}_1 + g_1\hat{i}_1\hat{k}_0), \tag{5.19}$$

and abbreviations

$$\begin{aligned}i_l &= i_l(\alpha), \qquad \hat{i}_l = i_l(\alpha x_1),\\ k_l &= k_l(\alpha), \qquad \hat{k}_l = k_l(\alpha x_1), \qquad l = 0, 1.\end{aligned} \tag{5.20}$$

From Eq. (3.14) we find for the Fourier transform of the correlation function

$$\hat{C}_A(\omega) = 4\pi a^3 g_0\tau_0\left[\frac{1}{3\alpha^2} + X_0\frac{i_1}{\alpha}\right]. \tag{5.21}$$

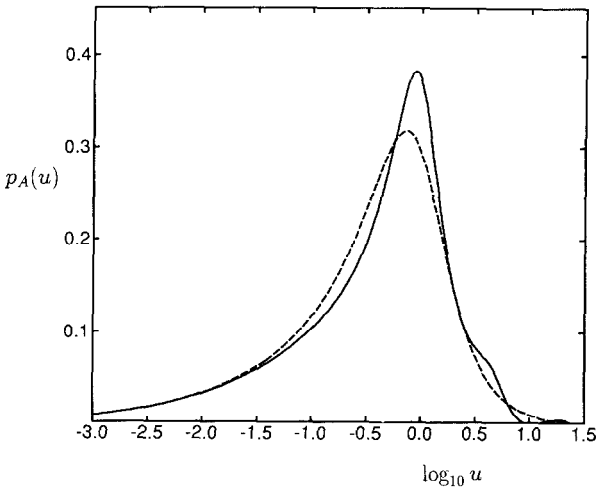

Fig. 1. Plot of the spectral density $p_A(u)$ as a function of $\log_{10} u$ for the single barrier model with parameters $g_0 = 1.2$, $g_1 = 0.8$, $x_1 = 2$ (drawn curve). We compare with the spectral density $p_{A2}(u)$ found in two-pole approximation (dashed curve).

From Eq. (2.19) we find the Laplace transform

$$\Gamma_A(z) = \frac{\tau_0}{\tau_M}\left[\frac{1}{\alpha^2} + 3X_0\frac{i_1}{\alpha}\right] \tag{5.22}$$

with

$$\alpha = \sqrt{\tau_0 z/\tau_M}. \tag{5.23}$$

Hence we may find the exact spectral density by putting $\sqrt{z} = i\sqrt{u}$ and taking the imaginary part,

$$p_A(u) = \frac{-1}{\pi}\operatorname{Im}\Gamma_A(\sqrt{z} = i\sqrt{u}). \tag{5.24}$$

The relaxation function $\gamma_A(\tau)$ may be found from Eq. (2.17) by numerical integration.

In Fig. 1 we plot the exact spectral density $p_A(u)$ as a function of $\log_{10} u$ for the choice of parameters $g_0 = 1.2$, $g_1 = 0.8$, and $x_1 = 2$. We compare with the two-pole approximation $p_{A2}(u)$, as given by Eq. (5.2) with parameter σ given by Eqs. (5.9) and (5.11). In this example the mean relaxation time is $\tau_M = 1.292\,\tau_{M0}$, and the width parameter takes the value $\sigma = 1.077$. The mean exit time is $\tau_{e1} = 1.625\,\tau_{M0}$. The spectral density spans several decades, and the two-pole approximation is fairly good.

In Fig. 2 we plot the spectral density $p_A(u)$ for the choice of parameters $g_0 = 2$, $g_1 = 0.2$, and $x_1 = 2$. We compare again with the two-pole approximation. In this example the mean relaxation time is $\tau_M = 5.167\,\tau_{M0}$, and the width parameter takes the value $\sigma = 0.224$. The mean exit time happens to be the same as τ_M. The spectrum is much narrower than in the previous example, and the two-pole approximation is less satisfactory.

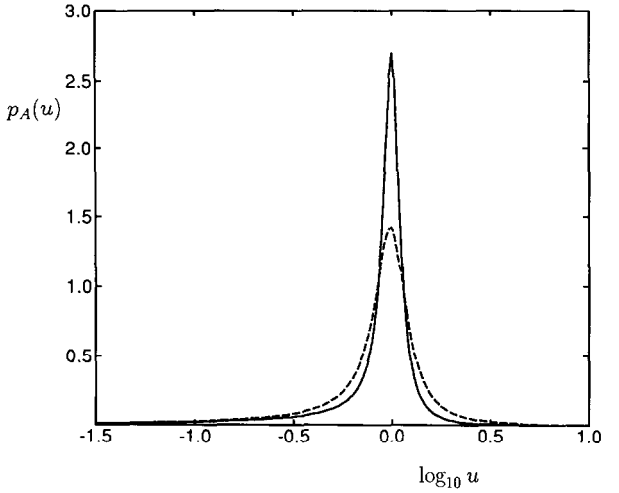

Fig. 2. Same as in Fig. 1 with parameters $g_0 = 2$, $g_1 = 0.2$, $x_1 = 2$.

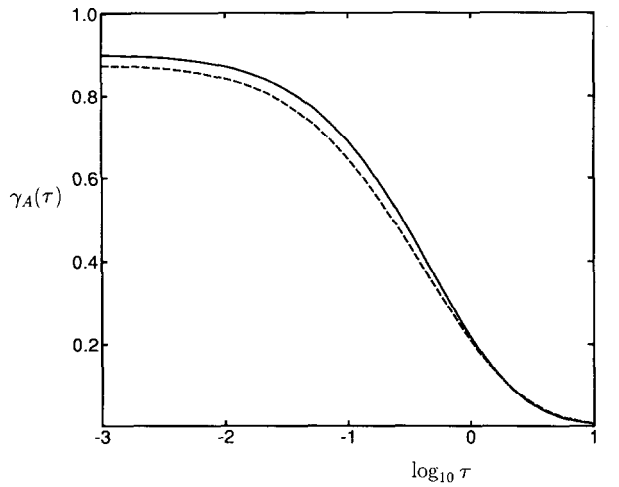

Fig. 3. Plot of the relaxation function $\gamma_A(\tau)$ as a function of $\log_{10} \tau$ for the single barrier model with parameters as in Fig. 1 (drawn curve). We compare with the function predicted in two-pole approximation (dashed curve).

In Fig. 3 we plot the exact relaxation function $\gamma_A(\tau)$ against $\log_{10}\tau$ for the choice of parameters $g_0 = 1.2$, $g_1 = 0.8$, and $x_1 = 2$. We compare with the function $\gamma_{A2}(\tau)$, as found from the two-pole spectrum. In Fig. 4 we plot the functions for the choice of parameters $g_0 = 2$, $g_1 = 0.2$, and $x_1 = 2$. In both cases there is qualitative agreement between the exact relaxation function and the two-pole approximation, especially at long times, but there are significant deviations at short times.

In two-pole approximation the relaxation function is given by the closed expression

$$\gamma_{A2}(\tau) = A_+ w(-iy_+\sqrt{\tau}) + A_- w(-iy_-\sqrt{\tau}), \tag{5.25}$$

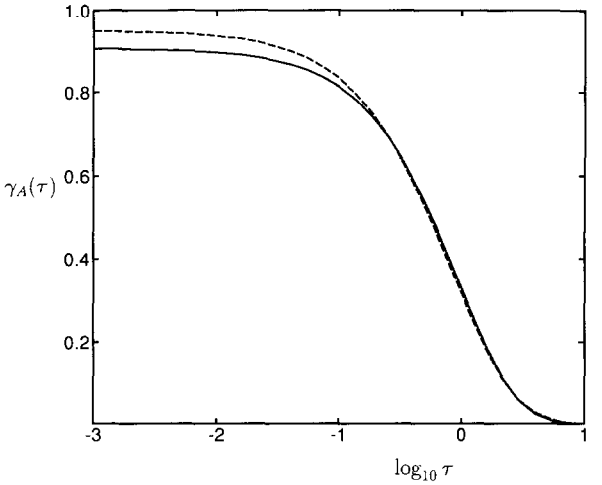

Fig. 4. Same as in Fig. 3 with parameters as in Fig. 2.

where $w(z)$ is related to the error function of complex argument [27]. The values $y_\pm$ correspond to the roots $z_\pm$ of the denominator in Eq. (5.1) as $y_\pm = \sqrt{z_\pm}$ and are given by

$$y_\pm = -\tfrac{1}{2}\sigma \pm \tfrac{1}{2}\sqrt{\sigma^2 - 4}. \tag{5.26}$$

The amplitudes $A_\pm$ are given by

$$A_\pm = \frac{\pm y_\pm}{y_+ - y_-}. \tag{5.27}$$

For the single barrier model the correlation function is characterized by a broad relaxation spectrum, which is fairly well approximated by a two-pole approximation. Qualitatively the relaxation spectrum consists of a single broad peak. It is clear that the approximation has its limitations and that more complicated relaxation processes require a more sophisticated treatment.

6. Double barrier

In this section we investigate how the presence of a second barrier affects the relaxation process. In order to perform explicit calculations we consider a model with a piecewise constant potential,

$$\begin{aligned} v(r) &= v_0 \quad \text{for} \quad 0 < r < a, \\ &= v_1 \quad \text{for} \quad a < r < b_1, \\ &= v_2 \quad \text{for} \quad b_1 < r < b_2, \\ &= v_3 \quad \text{for} \quad b_2 < r < b_3, \end{aligned}$$

$$= 0 \qquad \text{for} \qquad b_3 < r. \tag{6.1}$$

We study again the correlation function $C_A(t)$ for the function $A(r) = \theta(a - r)$. First we must find the steady-state solution $f^{(0)}(r)$. With the notation $x_j = b_j/a$ and $g_j = \exp(-\beta v_j)$ the jump conditions at x_j take the form (5.6), now for $j = 0, 1, 2, 3$. The solution has a form similar to that in Eq. (5.7). The mean relaxation time τ_M is given by the expression (5.9), but now with the coefficient

$$X_0^{(0)} = \tfrac{1}{6} + \frac{g_0}{3g_1}\frac{x_1 - 1}{x_1} + \frac{g_0}{3g_2}\frac{x_2 - x_1}{x_1 x_2} + \frac{g_0}{3g_3}\frac{x_3 - x_2}{x_2 x_3} + \frac{g_0}{3x_3}. \tag{6.2}$$

The "charge" Q_A and the width parameter σ are again given by the expressions (5.9) and (5.11).

The mean exit time can be calculated for any chosen spherical surface. For the sphere with radius b_1+ we find again the expression (5.15). This is not affected by the presence of the second barrier. A second mean exit time of interest is defined for a sphere with radius b_3+, just outside the second barrier. The solution of the steady state Eq. (5.13) on the interval $0 < x < x_3+$ with absorbing boundary condition at x_3+ takes the form

$$f_e(x) = \left[X_0^{(e)} - \tfrac{1}{6}x^2\right]\tau_0 \qquad \text{for } 0 < x < 1, \tag{6.3}$$

with the rather complicated coefficient

$$X_0^{(e)} = \tfrac{1}{6}x_3^2 + \frac{g_2 - g_3}{3g_3}\frac{x_2^2(x_3 - x_2)}{x_3} + \frac{g_1 - g_2}{3g_3}\frac{x_1^3(x_3 - x_2)}{x_2 x_3} + \frac{g_1 - g_2}{3g_2}\frac{x_1^2(x_2 - x_1)}{x_2} + \frac{(g_1 - g_2)(g_0 - g_1)}{3g_1 g_2 x_1} + \frac{g_0 - g_1}{3g_3}\frac{x_3 - x_2}{x_2 x_3} - \frac{g_0 - g_1}{3g_2 x_2} + \frac{g_0 - g_1}{3g_1}. \tag{6.4}$$

The expression in Eq. (6.3) is the average time it takes a particle starting at radius $r = xa$ to diffuse for the first time through the sphere of radius b_3+, just outside the second barrier. Averaging over the sphere of radius a we find the mean exit time

$$\tau_{e3} = \left[X_0^{(e)} - \tfrac{1}{10}\right]\tau_0. \tag{6.5}$$

It is clear that the two mean exit times τ_{e1} and τ_{e3} can be quite different, depending on the various heights and widths.

The correlation function $C_A(t)$ can be evaluated exactly, by the same method as for the single barrier. The radial distribution function $\hat{f}(x, \alpha)$ is given by an expression like Eq. (5.16), with constant coefficients X_j, Y_j on each interval where the potential is constant. The Laplace transform $\Gamma_A(z)$ of the relaxation function is given by Eq. (5.22) with the appropriate value for the coefficient $X_0(\alpha)$. The spectral density $p_A(u)$ is found from Eq. (5.24).

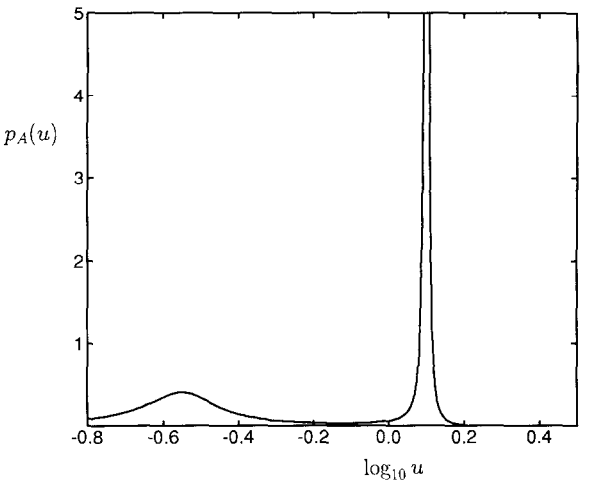

Fig. 5. Plot of the spectral density $p_A(u)$ as a function of $\log_{10} u$ for the double barrier model with parameters $g_0 = 2$, $g_1 = 0.2$, $g_2 = 2$, $g_3 = 0.2$, $x_1 = 2$, $x_2 = 3$, $x_3 = 4$.

As a specific example we consider the case with parameters $g_0 = 2$, $g_1 = 0.2$, $g_2 = 2$, $g_3 = 0.2$, $x_1 = 2$, $x_2 = 3$, $x_3 = 4$, corresponding to two wells of equal depth and two barriers of equal height. In this case the mean relaxation time is $\tau_M = 5.583\tau_{M0}$, and the width parameter takes the value $\sigma = 0.200$. The mean exit time for the first barrier takes the value $\tau_{e1} = 5.167\tau_{M0}$, whereas the mean exit time for the second barrier equals $\tau_{e3} = 21.792\tau_{M0}$. This shows that there are at least two distinct time scales in the problem, one for passage across the first barrier, and one for passage across both barriers.

In Fig. 5 we plot the exact spectral density for the above choice of parameters. There are two distinct peaks, a narrow one which can be associated with the fast escape across the first barrier, and a broader one which corresponds to the slower passage across both barriers. The sharp peak has its maximum 26.97 at $u = 1.262$. The broad peak has its maximum 0.405 at $u = 0.281$. It is clear that the two-pole approximation discussed in the preceding section cannot provide an adequate description.

7. Rational approximation

In previous articles we have improved on the two-pole approximation by considering a four-pole approximation [28,29]. However, it turns out that the method is not adequate for the spectrum shown in Fig. 5. The sharp features of the spectrum require a more sophisticated treatment. We have conjectured previously [21] that in problems of diffusion the Laplace transform $\Gamma(z)$ of a typical relaxation function $\gamma(\tau)$ can be represented by a meromorphic function in the $\sqrt{z}$ plane. The conjecture is supported by the exact solution for the function $\Gamma_A(z)$ for the models discussed in the preceding two sections. Since usually one is not interested in the detailed behavior of the relaxation

function $\gamma(\tau)$ for very short times, it is not necessary to know the Laplace transform $\Gamma(z)$ in full detail. Rather, it suffices to approximate $\Gamma(z)$ by a rational function of $\sqrt{z}$, i.e. by a ratio of two polynomials in $\sqrt{z}$, chosen such that it provides an accurate description in a limited range of $|\sqrt{z}|$ around $z = 0$.

The rational approximation can be constructed by the method of N-point Padé approximants (NPP) [24,25]. This requires knowledge of the function to be approximated at N points in the complex plane. We shall choose points lying on the positive z axis. By definition the function $\Gamma_A(z)$ is real on the positive z axis. As a consequence the approximation is constructed with real numbers, which has computational advantage. We have found in our examples that the method quickly leads to precise results.

We write the exact Laplace transform $\Gamma_A(z)$ in the form

$$\Gamma_A(z) = \frac{1}{1 + \sigma\sqrt{z} + z + z\psi(\sqrt{z})}, \tag{7.1}$$

where $\psi(\sqrt{z})$ tends to a constant for $z \to 0$ and to zero for $z \to \infty$. These conditions guarantee that Eq. (2.22) is satisfied, and that the first two terms in the expansion in powers of $\sqrt{z}$ agree with the first two terms in the expansion (4.2). We denote the rational approximant which uses $p + 1$ points as $\Gamma_A^{(p+1)}(z)$. It takes the form

$$\Gamma_A^{(p+1)}(z) = \frac{1}{1 + \sigma\sqrt{z} + z + z\psi_p(\sqrt{z})}, \tag{7.2}$$

where $\psi_p(\sqrt{z})$ is a ratio of two polynomials in $y = \sqrt{z}$,

$$\psi_p(y) = \frac{A_p(y)}{B_p(y)}. \tag{7.3}$$

Here A_p and B_p are polynomials of degree $\frac{1}{2}p$ for p even, whereas A_p is of degree $\frac{1}{2}(p-1)$ and B_p is of degree $\frac{1}{2}(p+1)$ for p odd. The coefficients in the polynomials are determined by Thiele's reciprocal-difference method [30]. Let $y_0, \ldots, y_p$ be the $p + 1$ points at which $\psi_p(y)$ is fitted to $\psi(y)$. We write $\psi_p(y)$ as the continued fraction

$$\psi_p(y) = \cfrac{a_0}{1 + \cfrac{(y - y_0)a_1}{1 + \cfrac{(y - y_1)a_2}{1 + \cfrac{\cdots}{1 + \cfrac{\cdots}{1 + \cfrac{(y - y_{p-2})a_{p-1}}{1 + (y - y_{p-1})a_p}}}}}}. \tag{7.4}$$

The coefficients $a_0, \cdots, a_p$ are determined successively from the equations

$$a_0 = \psi(y_0),$$

$$a_1 = \frac{[\psi(y_0)/\psi(y_1)] - 1}{y_1 - y_0},$$

$$a_j = \frac{1}{y_{j-1} - y_j}\left[1 + \cfrac{(y_j - y_{j-2})a_{j-1}}{1 + \cfrac{(y_j - y_{j-3})a_{j-2}}{1 + \cfrac{\cdots}{1 + \cfrac{\cdots}{1 + \cfrac{(y_j - y_0)a_1}{1 - [\psi(y_0)/\psi(y_j)]}}}}}\right], \quad j = 2, \ldots, p. \tag{7.5}$$

The polynomials A_p and B_p follow from the recursion relations

$$A_{n+1} = A_n + (y - y_n)a_{n+1}A_{n-1},$$
$$B_{n+1} = B_n + (y - y_n)a_{n+1}B_{n-1}, \tag{7.6}$$

with initial values

$$A_{-1} = 0, \qquad A_0 = a_0,$$
$$B_{-1} = 1, \qquad B_0 = 1. \tag{7.7}$$

The resulting ratio $\psi_p(y)$ does not depend on the order of the chosen points. Convergence can be optimized by a proper choice of points. In our examples the set of points

$$y_j = \frac{\sqrt{j+1}}{p - j + 1}, \qquad j = 0, \ldots, p \tag{7.8}$$

leads to rapid convergence. We have not found it advantageous to include information on further terms in the expansion (4.2).

For the example treated at the end of Section 6 it suffices to fit at the ten points given by Eq. (7.8) for $p = 9$ to get excellent agreement for the spectrum. If the spectrum shown in Fig. 5 is calculated from the rational approximation, it cannot be distinguished from the exact spectrum on the scale of the figure.

8. Dominant poles

The rational approximation which we have constructed in the preceding section allows a simplified representation of the exact spectrum $p_A(u)$, which is accurate over a wide range of u. Deviations become appreciable for large values of u, but these correspond to very fast relaxation, which is usually not of interest. The behavior of the relaxation function $\gamma_A(\tau)$, as given by Eq. (2.17), is described very well by the approximate spectrum. Further analysis shows that the function is dominated by a relatively small number of poles of $\Gamma_A(z)$ in the $\sqrt{z}$ plane. The location of the dominant poles and their residues can be determined accurately from the rational approximation.

We write

$$\Gamma_A(z) = \sum_j \frac{R_j}{y - y_j}, \tag{8.1}$$

with $y = \sqrt{z}$, poles y_j, and residues R_j. The poles occur either in conjugate pairs (y_j, y_j^*) with negative real part y_j', and with residues (R_j, R_j^*), or singly on the negative real axis. From the analytic form of the function $\Gamma_A(z)$, as given in Eq. (7.1), it follows that the poles and residues satisfy the sum rules

$$\begin{aligned} \sum_j R_j y_j &= 1, & \sum_j R_j &= 0, \\ \sum_j \frac{R_j}{y_j} &= -1, & \sum_j \frac{R_j}{y_j^2} &= \sigma. \end{aligned} \tag{8.2}$$

The first two sum rules follow from the behavior of $\Gamma_A(z)$ for large z, the second two from the behavior for small z. Taking the inverse Laplace transform in Eq. (8.1), using the variable $v = -iy$, and shifting the contour of integration we find for the relaxation function

$$\gamma_A(\tau) = \frac{1}{\pi} \int_{-\infty}^{\infty} \sum_j \frac{R_j}{v + iy_j} e^{-v^2\tau} v \, dv. \tag{8.3}$$

Using the second sum rule in Eq. (8.2) we can transform to

$$\gamma_A(\tau) = \frac{-i}{\pi} \int_{-\infty}^{\infty} \sum_j \frac{R_j y_j}{v + iy_j} e^{-v^2\tau} \, dv. \tag{8.4}$$

Hence the relaxation function is given by [27]

$$\gamma_A(\tau) = \sum_j R_j y_j \, w\left(-iy_j\sqrt{\tau}\right). \tag{8.5}$$

The second set of sum rules (8.2) must be satisfied to good approximation by the dominant poles. If we denote the set of dominant poles by D, then we must have

$$\sum_{d\in D} \frac{R_d}{y_d} \approx -1, \qquad \sum_{d\in D} \frac{R_d}{y_d^2} \approx \sigma. \tag{8.6}$$

We define

$$\begin{aligned} W_d &= -\tfrac{1}{2}\left(\frac{R_d}{y_d} + \frac{R_d^*}{y_d^*}\right), & S_d &= \tfrac{1}{2}\left(R_d y_d + R_d^* y_d^*\right), \\ L_d &= \frac{1}{2\sigma}\left(\frac{R_d}{y_d^2} + \frac{R_d^*}{y_d^{*2}}\right). \end{aligned} \tag{8.7}$$

Here W_d gives the contribution of pole d to the time integral of $\gamma_A(\tau)$, i.e. to $\Gamma_A(0) = 1$, and S_d gives its contribution to the initial value $\gamma_A(0) = 1$. Furthermore, L_d gives the

relative contribution of pole d to the coefficient of the long-time decay. The contributions W_d, S_d, and L_d can be positive or negative. For the set of dominant poles one must have

$$\sum_{d\in D} W_d \approx 1, \qquad \sum_{d\in D} L_d \approx 1. \tag{8.8}$$

The sum of short-time coefficients S_d determines the jump Γ_∞ from unity in the initial decay

$$\Gamma_\infty = 1 - \sum_{d\in D} S_d. \tag{8.9}$$

The relaxation function $\gamma_A(\tau)$ is given to good approximation by

$$\gamma_A(\tau) \approx \sum_{d\in D} R_d\, y_d\, w\left(-iy_d\sqrt{\tau}\right). \tag{8.10}$$

As an example we consider a two barrier problem with wells of zero depth. We study first the case with parameters $g_0 = 1$, $g_1 = 0.2$, $g_2 = 1$, $g_3 = 0.2$, $x_1 = 2$, $x_2 = 3$, $x_3 = 4$. In this case the mean relaxation time is $\tau_M = 2.944\tau_{M0}$, and the width parameter takes the value $\sigma = 0.261$. The mean exit time for the first barrier is $\tau_{e1} = 3.083\tau_{M0}$, and that for the second one $\tau_{e3} = 12.861\tau_{M0}$. Comparison with the corresponding values for the model studied in Section 6 shows that the depth of the wells has an appreciable influence, as one would expect. In Fig. 6 we plot the exact spectral density $p_A(u)$ for the above choice of parameters. Qualitatively the spectrum is very similar to that in Fig. 5. The sharp peak has its maximum 18.43 at $u = 1.184$. The broad peak has its maximum 0.469 at $u = 0.285$. The peaks broaden as the height of the barriers is lowered. The rational approximation gives a spectrum which cannot be distinguished from the exact one on the scale of the figure. In Table 1 we list the dominant poles $\{y_d\}$ in the y plane, as well as their residues $\{R_d\}$. We also list the coefficients $\{W_d, S_d, L_d\}$, as defined in Eq. (8.7), and as calculated from the rational approximation with $p = 11$. It can be seen that the sum rules (8.8) are very well satisfied. The jump Γ_∞, defined in Eq. (8.9), vanishes. In Fig. 7 we plot the relaxation function $\gamma_A(\tau)$, as given by Eq. (8.10). Only the single pole indicated by $d = 2$ and the pairs (3,4), (5,6), (7,8) contribute appreciably.

In our second example we consider the same heights and depths as in the preceding case, but broaden the barriers and the second well. We choose the parameters $g_0 = 1$, $g_1 = 0.2$, $g_2 = 1$, $g_3 = 0.2$, $x_1 = 3$, $x_2 = 5$, $x_3 = 7$. In this case the mean relaxation time is $\tau_M = 3.413\tau_{M0}$, and the width parameter takes the value $\sigma = 0.209$. The mean exit time for the first barrier is $\tau_{e1} = 5.722\tau_{M0}$, and that for the second one $\tau_{e3} = 38.935\tau_{M0}$. In Fig. 8 we plot the exact spectral density $p_A(u)$ and the approximate one found from the rational approximation with $p = 11$. In this case one sees a difference between the two spectra for high relaxation rates, but this will have little influence on the relaxation function in the intermediate and long time regime. The sharp peak has its maximum 80.13 at $u = 0.795$. The broad peak for small u has its maximum 0.224 at $u = 0.102$. In Table 2 we list the dominant poles $\{y_d\}$, their residues $\{R_d\}$, and the coefficients

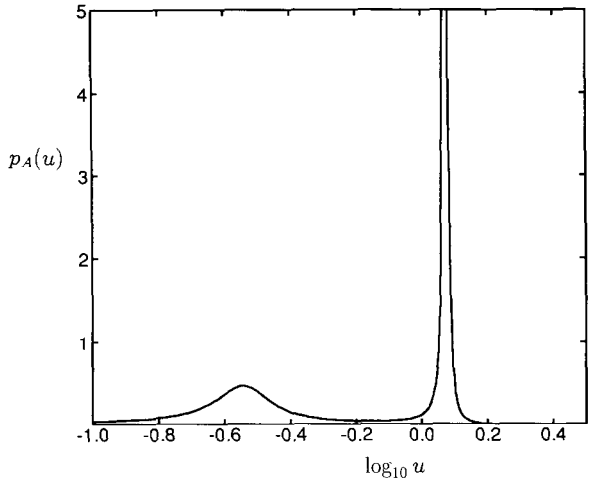

Fig. 6. As in Fig. 5 with parameters $g_0 = 1$, $g_1 = 0.2$, $g_2 = 1$, $g_3 = 0.2$, $x_1 = 2$, $x_2 = 3$, $x_3 = 4$.

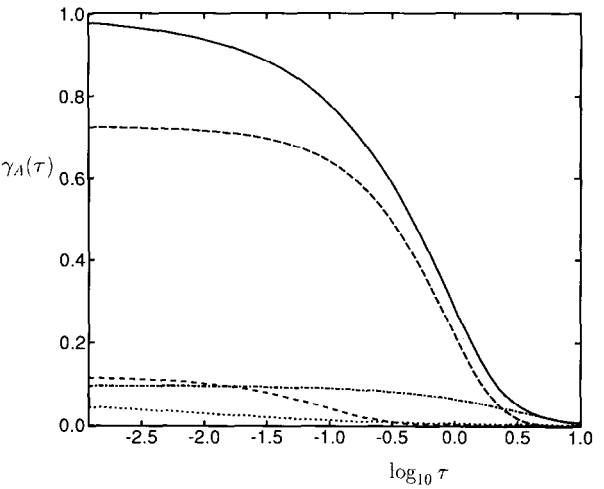

Fig. 7. Plot of the relaxation function $\gamma_A(\tau)$ as a function of $\log_{10} \tau$ for the double barrier model with parameters as in Fig. 6 (drawn curve). We also show the contribution from the single pole y_2 (dotted curve), from the pair of poles (y_3, y_4) (dash-dotted curve), from the pair (y_5, y_6) (long dashes), and from the pair (y_7, y_8) (short dashes). The single pole y_1 gives a small negative contribution, not visible on the scale of the figure.

$\{W_d, S_d, L_d\}$. The sum rules (8.8) are very well satisfied. The jump Γ_∞ vanishes. In Fig. 9 we plot the relaxation function $\gamma_A(\tau)$, as given by Eq. (8.10). Only the single pole indicated by $d = 2$ and the pairs (3,4), (5,6), (7,8) contribute appreciably.

Table 1
Characteristics of the rational approximation for the double barrier model with Boltzmann factors $g_0 = 1$, $g_1 = 0.2$, $g_2 = 1$, $g_3 = 0.2$, and steps at $x_0 = 1$, $x_1 = 2$, $x_2 = 3$, $x_3 = 4$

d	y'	y''	R'	R''	$(2)W$	$(2)S$	$(2)L$
1	-0.315	0	0.011	0	0.036	-0.004	0.437
2	-8.645	0	-0.007	0	-0.001	0.059	0
3	-0.063	0.533	0.003	-0.091	0.337	0.097	0.484
5	-0.006	1.088	-0.009	-0.334	0.614	0.728	0.080
7	-0.326	3.055	0.004	-0.020	0.013	0.200	0.001

We list the real and imaginary parts y'_d, y''_d of the poles in the complex y plane for $d = 1, 2, 3, 5, 7$, together with the real and imaginary parts R'_d, R''_d of their residues. The poles for $d = 3, 5, 7$ have complex conjugates y_4, y_6, y_8 with corresponding complex conjugate residues R_4, R_6, R_8. In the sixth column we list the weight W_d for the real poles, and $2W_d$ for the members of a conjugate pair. Similarly in the seventh and eighth columns we list the short-time coefficients $(2)S_d$ and the long-time coefficients $(2)L_d$.

Table 2
As in Table 1 for the double barrier model with Boltzmann factors $g_0 = 1$, $g_1 = 0.2$, $g_2 = 1$, $g_3 = 0.2$, and steps at $x_0 = 1$, $x_1 = 3$, $x_2 = 5$, $x_2 = 7$

d	y'	y''	R'	R''	$(2)W$	$(2)S$	$(2)L$
1	-0.193	0	0.004	0	0.019	-0.001	0.460
2	-2.680	0	-0.048	0	-0.018	0.128	-0.032
3	-0.034	0.319	-0.001	-0.024	0.147	0.015	0.536
5	-0.001	0.893	-0.005	-0.339	0.760	0.607	0.067
7	-0.196	1.707	0.028	-0.077	0.093	0.251	-0.032

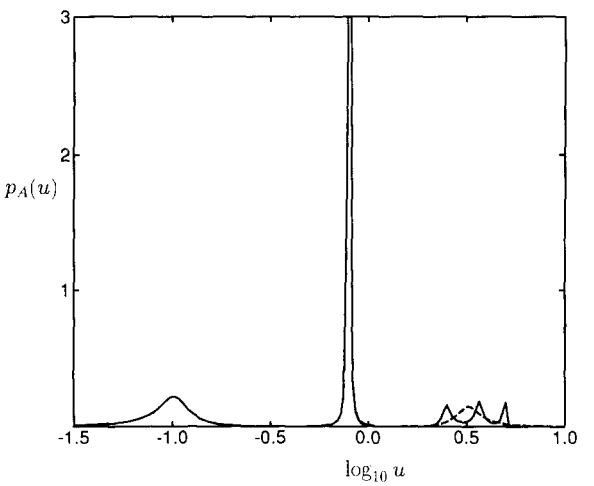

Fig. 8. As in Fig. 5 with parameters $g_0 = 1$, $g_1 = 0.2$, $g_2 = 1$, $g_3 = 0.2$, $x_1 = 3$, $x_2 = 5$, $x_3 = 7$ (drawn curve). We compare with the spectral density as found in rational approximation with eight poles (dashed curve).

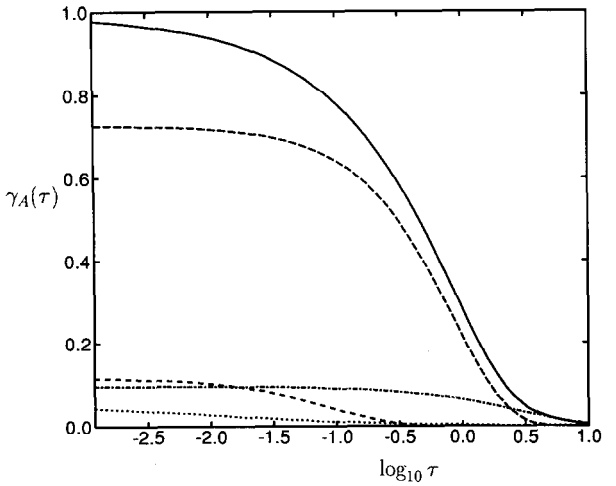

Fig. 9. As in Fig. 7 for the double barrier model with parameters as in Fig. 8.

9. Loss spectrum

In the preceding sections we have concentrated on the relaxation spectrum $p_A(u)$, since this fully determines the linear relaxation system. On the other hand, in experiment the relaxation spectrum is not determined directly, but must be found from the measured absorption spectrum, or from other data. We define the loss spectrum as the imaginary part of $\Gamma_A(z)$ for real ω,

$$s_A(\varpi) = \Gamma_A''(-i\varpi) = \varpi \int_0^\infty \frac{p_A(u)}{u^2+\varpi^2}\,du\,, \tag{9.1}$$

with the dimensionless variable $\varpi = \omega\tau_M$. It has been shown by Roesler and Pearson [31] that the relation between the relaxation spectrum $p_A(u)$ and the loss spectrum $s_A(\varpi)$ is particularly simple, when both are plotted on a logarithmic scale. We define

$$\bar{p}_A(\ln u) = p_A(u), \qquad \bar{s}_A(\ln\varpi) = s_A(\varpi). \tag{9.2}$$

The relation between the two functions $\bar{p}_A$ and $\bar{s}_A$ is given by a convolution integral

$$\bar{s}_A(x) = \tfrac{1}{2}\int_{-\infty}^{\infty} \operatorname{sech}(x-x')\bar{p}_A(x')dx'. \tag{9.3}$$

Hence one can easily find one from the other by taking Fourier transforms

$$\hat{\bar{s}}_A(\xi) = \int \exp(i\xi x)\bar{s}_A(x)dx,$$

$$\hat{\bar{p}}_A(\xi) = \int \exp(i\xi x)\bar{p}_A(x)dx. \tag{9.4}$$

The two transforms are related by

$$\hat{s}_A(\xi) = \frac{\pi}{2} \operatorname{sech} \tfrac{1}{2}\pi\xi \cdot \hat{p}_A(\xi). \tag{9.5}$$

Hence in principle one can find the relaxation spectrum exactly from the loss spectrum [31–33]. In practice the procedure shows instability. Fine details of the relaxation spectrum get lost, if the loss spectrum is known only approximately.

Alternatively one may use the method of N-point Padé approximants. The required values on the positive y axis may be found from the loss spectrum by use of the relation

$$\Gamma_A(z) = \frac{2}{\pi} \int_0^\infty \frac{\varpi}{\varpi^2 + z^2} s_A(\varpi) d\varpi, \qquad y = \sqrt{z}, \tag{9.6}$$

valid for $z > 0$. Hence one finds the spectrum $p_A(u)$ by use of the method discussed in the preceding sections.

The required values of $\Gamma_A(z)$ for positive z may also be found from other experimental data. For example, one may use the real part of the susceptibility for real frequency, rather than the imaginary part. If the time correlation function is measured directly, as in photon correlation spectroscopy [34], then one may use the time integral in Eq. (2.20).

10. Viscoelastic relaxation spectrum of polyisobutylene

As a demonstration of our method we consider the determination of the viscoelastic relaxation spectrum of polyisobutylene, a typical rubber-like high polymer [35]. We use data obtained by Marvin [36] for the imaginary part of the dynamic shear modulus of polyisobutylene at 25^0C, as listed by Roesler and Pearson [31].

The dynamic shear modulus $G(\omega)$ is related to the dynamic viscosity $\eta(\omega)$ by

$$G(\omega) = -i\omega\eta(\omega). \tag{10.1}$$

Both quantities have real and imaginary parts defined by

$$G(\omega) = G'(\omega) - iG''(\omega), \qquad \eta(\omega) = \eta'(\omega) + i\eta''(\omega). \tag{10.2}$$

At high frequency the shear modulus tends to the real value G_∞. Roesler and Pearson [31] list 24 data points for the imaginary part $G''(\omega)$, spanning a wide range of frequency. However, only about 8 data points turn out to be relevant for a determination of the relaxation spectrum. For the other points the reduced real part of the viscosity $\eta'(\omega)/\eta(0)$ equals either unity, or almost zero. Nonetheless the data turn out to be sufficient for an application of our method.

First we determine the zero frequency viscosity $\eta(0)$ by extrapolation of the low frequency data. This yields the value $\eta(0) = 1.45 \times 10^{18}$ dyne cm$^{-2}/[\omega]$, where $[\omega]$ is the unit of frequency, which is not specified by Roesler and Pearson [31]. Next we determine the high-frequency shear modulus G_∞, using the relation

$$G_\infty = \frac{2}{\pi}\int_0^\infty \frac{G''(\omega)}{\omega}\,d\omega, \tag{10.3}$$

and approximating the integral by a sum. This yields the value $G_\infty = 1.35 \times 10^{10}$ dyne cm^{-2}. Hence we find the mean relaxation time $\tau_M = \eta(0)/G_\infty = 1.07 \times 10^{-8}/[\omega]$. Next we use the relation

$$\eta(i\omega'') = \frac{2\omega''}{\pi}\int_0^\infty \frac{G''(\omega)}{\omega(\omega^2+\omega''^2)}\,d\omega \tag{10.4}$$

to calculate $\eta(i\omega'')$ for positive ω''. It is convenient to rewrite this expression for low frequency in the form

$$\bar\eta(i\omega'') = 1 + \frac{2\omega''}{\pi}\int_0^\infty \frac{\bar\eta'(\omega)-1}{\omega^2+\omega''^2}\,d\omega, \tag{10.5}$$

where $\bar\eta(\omega) = \eta(\omega)/\eta(0)$ is the reduced dynamic viscosity. In this manner the leading contribution at low frequency is separated off. The integrals in Eqs. (10.4) and (10.5) can be calculated approximately from the data. The resulting values for $\bar\eta(i\omega'')$ should match for intermediate values of ω''. This does not quite happen, due to the paucity of data points.

The function $\bar\eta(-i\omega\tau_M)$ is the one-sided Fourier transform of the stress relaxation function. It can be identified with the Laplace transform $\Gamma_A(z)$ in Eq. (7.1). The parameter σ in Eq. (7.1) can be determined from the behavior of the reduced viscosity $\bar\eta(-i\omega\tau_M)$ for small positive imaginary ω. We find that the data can be fitted only with $\sigma = 0$. This shows that the dynamic viscosity has the analytic form postulated for the relaxation function $\Gamma(z)$ for colloidal suspensions of spheres [37]. The rational approximation to the function $\bar\eta(z)$ can be constructed by the method explained in Section 7, except that we cannot use the distribution of points given in Eq. (7.8), because of the mismatch at intermediate values of ω''. It turns out that the data are well represented by a four-pole approximation with two widely separated pairs of poles. We can determine their location and residues by choosing the points at values of $\sqrt{\omega''\tau_M}$ given by $j/(5-j)$ for $j = 1,2,3,4$. The poles and their residues are insensitive to small variations of the points.

In Table 3 we list the positions, residues, and the various coefficients obtained in four-pole approximation. The corresponding spectral density $p(u)$ is plotted in Fig. 10. Comparison with the figure of Roesler and Pearson [31] shows that our method provides better resolution. In addition we find the relaxation spectrum in a convenient analytic form. From the relaxation spectrum we can find the stress relaxation function $M_V(\tau)$, either by use of Eq. (8.10), or by integration, as shown in Eq. (2.17).

In Fig. 11 we plot the real and imaginary parts of the reduced dynamic viscosity, $\bar\eta'(\varpi)$ and $\bar\eta''(\varpi)$, as calculated from the four-pole approximation with parameters listed in Table III. The real part $\bar\eta'(\varpi)$ can be compared with the input data. It is

Table 3
Positions and residues of the poles y_1, y_3 for the four-pole approximation to the Laplace transform of the stress relaxation function of polyisobutylene

d	y'	y''	R'	R''	$2W$	$2S$
1	-0.06	0.49	0.07	-0.12	0.52	0.11
3	-0.4	1.2	-0.07	-0.35	0.48	0.89

The conjugate poles y_2 and y_4 have residues R_2, R_4, conjugate to R_1, R_3. We also list the weight $2W$ and the short-time coefficient $2S$ for each pair.

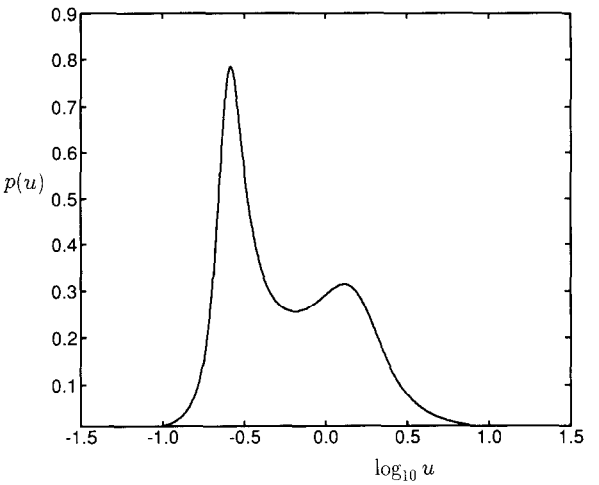

Fig. 10. Viscoelastic relaxation spectrum $p(u)$ of polyisobutylene as a function of $\log_{10} u$, as determined from data listed by Roesler and Pearson [31].

evident that we get an excellent fit. Finally, in Fig. 12 we plot the loss spectrum $s_V(\varpi) = \varpi\tilde{\eta}''(\varpi)$ as a function of $\log_{10}\varpi$. The two-peak structure of the relaxation spectrum gets lost due to the convolution shown in Eq. (9.3).

The above example shows that our method allows determination of the relaxation spectrum even from a rather small number of data. It will be of interest to analyze more complete data sets, obtained, for example, in dielectric and viscoelastic relaxation.

11. Discussion

We have developed a method for finding the relaxation spectrum of linear relaxation systems. We have tested the method in detail for a simple model of diffusion with one or two barriers. The analysis shows that the method works well, even in cases where the spectrum is broad, but has sharp features. We have used the method of N-point Padé approximants, a tool which has been applied successfully in the analysis of quantummechanical scattering amplitudes [24].

Our method has the advantage that the relaxation spectrum is found in a convenient

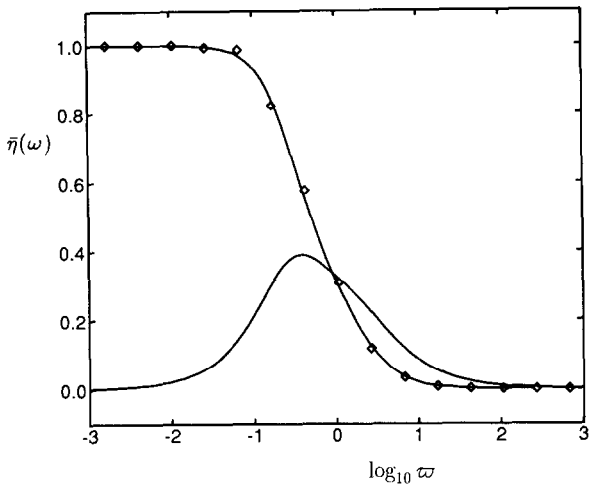

Fig. 11. Real and imaginary part of the reduced dynamic viscosity $\bar{\eta}(\omega) = \eta(\omega)/\eta(0)$ as a function of $\log_{10} \varpi$, where $\varpi = \omega\tau_M$, as calculated from the relaxation spectrum shown in Fig. 10. The real part is compared with the data listed by Roesler and Pearson [31].

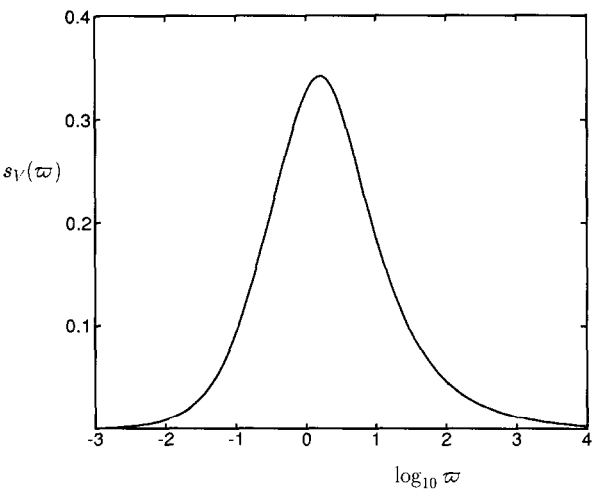

Fig. 12. Loss spectrum $s_V(\varpi) = \varpi\bar{\eta}''(\varpi)$ of polyisobutylene as a function of $\log_{10} \varpi$, as calculated from the relaxation spectrum shown in Fig. 10.

analytic form with numerical values for the parameters. This is demonstrated in our calculation of the viscoelastic relaxation spectrum of polyisobutylene from data which had been analyzed earlier by Roesler et al. [31–33]. It will be of particular interest to study the dependence of the relaxation spectrum on an external parameter, for example the temperature of a liquid near the glass transition [38]. We expect that the method will find many useful applications.

References

[1] H. König and J. Meixner, Math. Nachr. 19 (1958) 265.
[2] J. Meixner, Arch. Rational Mech. Anal. 17 (1964) 278.
[3] J. Meixner in Statistical Mechanics of Equilibrium and Non-Equilibrium, J. Meixner, ed. (North-Holland, Amsterdam, 1965).
[4] R. Kubo, J. Phys. Soc. Jpn. 12 (1957) 570.
[5] R. Kubo, M. Toda and N. Hashitsume, Statistical Physics II, Nonequilibrium Statistical Mechanics (Springer, Berlin, 1991).
[6] J. Meixner, J. Math. Phys. 4 (1963) 154.
[7] E.I. Takizawa and J. Meixner, J. Phys. Soc. Jpn. 35 (1973) 654.
[8] J.D. Ferry, Viscoelastic Properties of Polymers (Wiley, New York, 1970).
[9] C.J.F. Böttcher and P. Bordewijk, Theory of Electric Polarization, Vol. II (Elsevier, Amsterdam, 1978).
[10] W. Kauzmann, Chem. Rev. 43 (1948) 219.
[11] H. Eyring, J. Chem. Phys. 4 (1936) 283.
[12] H.A. Kramers, Physica 7 (1940) 284.
[13] C.W. Gardiner, Handbook of Stochastic Methods for Physics, Chemistry and the Natural Sciences (Springer, Berlin, 1983).
[14] N.G. van Kampen, Stochastic Processes in Physics and Chemistry (North-Holland, Amsterdam, 1992).
[15] P. Hänggi, P. Talkner and M. Borkovich, Rev. Mod. Phys. 62 (1990) 251.
[16] V.I. Mel'nikov, Phys. Rep. 209 (1991) 1.
[17] A.J. Barlow, A. Erginsav and J. Lamb, Proc. Roy. Soc. A 298 (1967) 481.
[18] G. Harrison, The Dynamic Properties of Supercooled Liquids (Academic, London, 1976).
[19] A.J. Barlow, A. Erginsav and J. Lamb, Proc. Roy. Soc. A 309 (1969) 473.
[20] R. Zwanzig, Physica A 118 (1983) 427.
[21] B. Cichocki and B.U. Felderhof, Phys. Rev. A 44 (1991) 6551.
[22] B. Cichocki and B.U. Felderhof, J. Chem. Phys. 96 (1992) 4669.
[23] B. Cichocki and K. Hinsen, Physica A 187 (1992) 133.
[24] R.W. Haymaker and L. Schlessinger, in: The Padé Approximant in Theoretical Physics, G.A. Baker, Jr. and J.L. Gammel, eds. (Academic, New York, 1970).
[25] G.A. Baker, Jr., Essentials of Padé Approximants (Academic, New York, 1975) Ch. 8.
[26] W. Feller, An Introduction to Probability Theory and its Applications, Vol. II (Wiley, New York, 1971) p. 439.
[27] Handbook of Mathematical Functions, edited by M. Abramowitz and I.A. Stegun (Dover, New York, 1965).
[28] B. Cichocki and B.U. Felderhof, J. Chem. Phys. 96 (1992) 9055.
[29] B. Cichocki and B.U. Felderhof, Langmuir 8 (1992) 2889.
[30] See L.M. Milne-Thomson, The Calculus of Finite Differences (Macmillan, New York, 1951).
[31] F.C. Roesler and J.R.A. Pearson, Proc. Phys. Soc. B 67 (1954) 338.
[32] F.C. Roesler, Proc. Phys. Soc. B 68 (1955) 89.
[33] F.C. Roesler and W.A. Twyman, Proc. Phys. Soc. B 68 (1955) 97.
[34] R. Pecora, ed., Dynamic Light Scattering and Velocimetry: Applications of Photon Correlation Spectroscopy (Plenum, New York, 1982).
[35] B. Frick, D. Richter and S. Trevino, Physica A 201 (1993) 88.
[36] R.S. Marvin, National Bureau of Standards, Report No. 2305 and addendum (1953).
[37] B. Cichocki and B.U. Felderhof, Phys. Rev. A 46 (1993) 7723.
[38] W. Götze, in: Liquids, Freezing and Glass Transition, J.P. Hansen, D. Levesque and J. Zinn-Justin, eds. (North-Holland, Amsterdam, 1991).